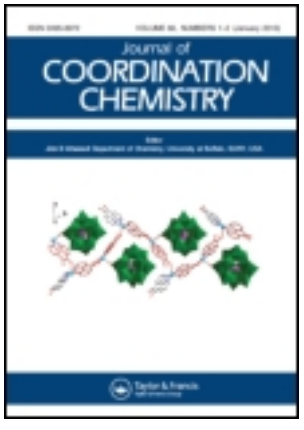

Journal of Coordination Chemistry
Publication details, including instructions for authors and subscription information:
http://www.tandfonline.com/loi/gcoo20

Synthesis, spectral, thermal analyses, molecular modeling, and antimicrobial activities of Cu(II)-complexes with 1,3,4-oxadiazole Schiff-base derivatives

Abdalla M. Khedr [a], Nadia A. El-Wakiel [a], Sudha Jadon [b] & Vipin Kumar [b]

[a] Department of Chemistry, Faculty of Science, Tanta University, Tanta, Egypt

[b] Department of Chemistry, Agra College, Agra-282002 (U.P.), India

Published online: 18 Feb 2011.

To cite this article: Abdalla M. Khedr, Nadia A. El-Wakiel, Sudha Jadon & Vipin Kumar (2011) Synthesis, spectral, thermal analyses, molecular modeling, and antimicrobial activities of Cu(II)-complexes with 1,3,4-oxadiazole Schiff-base derivatives, Journal of Coordination Chemistry, 64:5, 851-862, DOI: 10.1080/00958972.2011.557722

To link to this article: http://dx.doi.org/10.1080/00958972.2011.557722

Journal of Coordination Chemistry
Vol. 64, No. 5, 10 March 2011, 851–862

Synthesis, spectral, thermal analyses, molecular modeling, and antimicrobial activities of Cu(II)-complexes with 1,3,4-oxadiazole Schiff-base derivatives

ABDALLA M. KHEDR*†, NADIA A. EL-WAKIEL†,
SUDHA JADON‡ and VIPIN KUMAR‡

†Department of Chemistry, Faculty of Science, Tanta University, Tanta, Egypt
‡Department of Chemistry, Agra College, Agra-282002 (U.P.), India

(*Received 13 October 2010; in final form 3 December 2010*)

Seven Cu(II)-complexes with 2-amino-5-substituted aryl-1,3,4-oxadiazole Schiff bases are presented. The donors and possible geometries of the complexes were investigated by elemental and thermal (differential thermal analysis and thermogravimetric analysis) analyses, molar conductance, magnetic moments, IR, ^{1}H-NMR, ESR, UV-Vis, and mass spectra. The ligands are bidentate, coordinating through the nitrogen of azomethine and the nearest nitrogen to it. The results are supported by 3-D molecular modeling of **2** using CS Chem 3-D Ultra Molecular Modeling and Analysis Program. The investigated complexes have been screened for *in-vitro* antibacterial (*Escherichia coli* and *Staphylococcus aureus*) and antifungal (*Aspergillus flavus* and *Candida albicans*) activities. The qualitative and quantitative antimicrobial activities prove that the complexes are very active against the tested microorganisms.

Keywords: Cu(II)-complexes; Oxadiazole Schiff bases; Molecular modeling; Antimicrobial activity

1. Introduction

Various 1,3,4-oxadiazoles have been reported to possess analgesic [1], antihypertensive [2], antifungal [3], anti-inflammatory [4], and anticancer [5] activities. Schiff bases are an important class of compounds reported to possess various biological activities [6], including antibacterial [7], antifungal [8], anti-inflammatory [9], antipyretic [10], antitumor [11], and anticancer [12]. Also, Schiff bases are ligands in coordination chemistry [13]. Cu(II) forms a series of coordination compounds with well-defined structures and plays an important role in numerous biological processes that involve electron-transfer reactions or activation of some antitumor substances [14]. From the survey of existing literature [15–17], Cu(II)-complexes with Schiff bases have been used as biologically active complexes and as catalyst in chemical and petrochemical industries [18]. We continue our research [19, 20] on transition metal complexes with Schiff bases. This article presents the synthesis, characterization, and molecular

*Corresponding author. Email: abkhedr2001@yahoo.com

Journal of Coordination Chemistry
ISSN 0095-8972 print/ISSN 1029-0389 online
DOI: 10.1080/00958972.2011.557722

modeling of Cu(II)-complexes with Schiff bases (L^1–L^7) obtained by condensation of 2-amino-5-aryl-1,3,4-oxadiazole with different substituted aryl aldehydes (figure 1). Furthermore, we have tested the antibacterial and antifungal activities of the prepared complexes using strains of *Escherichia coli*, *Staphylococcus aureus*, *Aspergillus flavus*, and *Candida albicans*.

2. Experimental

The reagents used in this work were analytical grade products (Merck, Aldrich, or Sigma).

2.1. *Synthesis of the Schiff bases*

A solution of 2-amino-5-substituted aryl-1,3,4-oxadiazole (10 mmol) in ethanol (20 mL) was added to a solution of substituted aryl aldehyde (10 mmol) in 25 mL of ethanol. The mixture obtained was refluxed for 4–6 h. The volume of alcohol was reduced to half using a rotary evaporator. On cooling the reaction mixture, the precipitated Schiff base was filtered off, recrystallized from ethanol and dried in a vacuum desiccator over silica gel. The obtained Schiff bases, L^1–L^7 (figure 1), were subjected to melting point measurements, elemental, and spectral analyses to confirm their high purity [21].

2.2. *Synthesis of Cu(II)-complexes*

Complexes of Cu(II) were synthesized by the reflux-precipitation method. The hot ethanolic solution of ligand (1 mmol) was mixed with (249 mg, 1 mmol) hydrated cupric sulfate; the resulting mixture was refluxed for 4–6 h on a water bath. The solution was concentrated and the colored copper complex was precipitated. The complex was filtered, washed several times with hot water and cold ethanol to remove excess ligand and copper salt, and then dried in vacuum over anhydrous calcium chloride.

2.3. *Analysis and physical measurements*

Elemental analyses (for C, H, N) were done with a Perkin-Elmer 2400 elemental analyzer. Cu(II) content was estimated complexometrically using standard EDTA titration [22]. Molar conductance of the complexes was measured in DMF at room temperature using a conductance bridge of the type 523 conductometer. Mass spectral

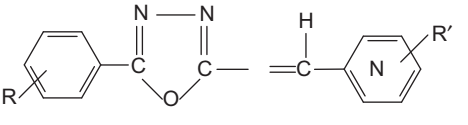

Figure 1. Ligand structures (L^1–L^7). R=R′=H (L^1), R=H, R′=4-NO_2 (L^2), R=3-Br, R′=3-Br (L^3), R=3-Cl, R′=3-Cl (L^4), R=4-F, R′=4-OH (L^5), R=3-NO_2, R′=3-NO_2 (L^6), R=4-OCH_3, R′=4-NO_2 (L^7).

measurements of the complexes were made on a Shimadzu LCMS-2010 eV mass spectrometer using the electron spray ionization (ESI) method at the Gakushuin University (Japan). Infrared (IR) spectra (KBr pellets) were recorded from 4000 to 400 cm^{-1} with a Perkin-Elmer (model 1430) IR spectrophotometer at the Microanalytical unit of Tanta University. ESR spectra were recorded on a Jeol spectrometer model JES-FE2XG equipped with an E101 microwave bridge. Measurements were done in the X band on microcrystalline powder at room temperature using DPPH as standard. ^{1}H-NMR spectra were recorded using a Bruker DMX 750 (500 MHz) spectrometer with DMSO-d_6 as solvent and TMS as internal standard. Magnetic measurements were carried out at room temperature by Gouy's method using magnetic susceptibility instrument (20 kG). Molar susceptibilities were corrected for diamagnetism of the component atoms applying Pascal's constants [23]. Electronic spectra were recorded using a Cary-400 double beam recording spectrophotometer within the wavelength range 190–700 nm. Differential thermal analysis (DTA) and thermogravimetric analysis (TGA) measurements were recorded on Shimadzu DT-50 and TG-50 thermal analyzers with heating rate of 10°C min^{-1}, from ambient temperature to 800°C.

2.4. *Molecular modeling studies*

The 3-D molecular modeling of a representative compound was carried out on a CS Chem 3-D Ultra Molecular Modeling and Analysis Program [24]. It is an interactive graphics program that allows rapid structure building, geometry optimization with minimum energy and molecular display. It has ability to handle transition metal complexes [25].

2.5. In-vitro *antibacterial and antifungal assay by the Kirby–Bauer method*

Antimicrobial activities of the tested samples were determined using a modified Kirby–Bauer disc diffusion method [26] at the microanalytical unit of Cairo University. Briefly, 100 μL of the test bacteria/fungi were grown in 10 mL of fresh media until they reached 10^6 cells mL^{-1} for bacteria or 10^5 cells mL^{-1} for fungi [27]. Hundred microliters of microbial suspension was spread onto agar plates corresponding to the broth in which they were maintained. Isolated colonies of each organism that might be playing a pathogenic role were selected from primary agar plates and tested for susceptibility by the disc diffusion method [28]. From the many media available, NCCLS recommends Mueller–Hinton agar since it results in good batch-to-batch reproducibility. The disc diffusion method for filamentous fungi used approved standard method (M38-A) developed by the NCCLS [29] for evaluating the susceptibilities of filamentous fungi to antifungal agents. The disc diffusion method for yeasts used approved standard method (M44-P) developed by the NCCLS [30]. Plates inoculated with filamentous fungi *A. flavus NRRL 6554* at 25°C for 48 h; Gram positive bacteria as *S. aureus NCTC 6356* and Gram negative bacteria as *E. coli NRRL-B-3704* were incubated at 35–37°C for 24–48 h and yeast *C. albicans ATCC 10231* was incubated at 30°C for 24–48 h, and then the diameters of the inhibition zones were measured in millimeters [31]. Standard discs of tetracycline (antibacterial agent) and amphotericin B (antifungal agent) served as positive controls for antimicrobial activity but filter discs impregnated with 10 μL of

solvent (distilled water or DMSO) were used as a negative control. The agar used is Meuller–Hinton agar that is rigorously tested for composition and pH. The depth of the agar in the plate is a factor to be considered in the disc diffusion method. This method is well-documented and standard zones of inhibition have been determined for susceptible and resistant values. Blank paper discs (Schleicher & Schuell, Spain) with a diameter of 8.0 mm were impregnated with 10 μL of tested concentration of the stock solutions. When a filter paper disc impregnated with a tested chemical is placed on agar the chemical diffuses from the disc into the agar, placing the chemical in the agar only around the disc. The solubility of the chemical and its molecular size will determine the size of the area of chemical infiltration around the disc. If an organism is placed on the agar it will not grow in the area around the disc if it is susceptible to the chemical. This area of no-growth around the disc is known as a "zone of inhibition" or "clear zone". For disc diffusion, the zone diameters were measured with slipping calipers of the National Committee for Clinical Laboratory Standards [31]. Agar-based methods such as E-test and disc diffusion can be good alternatives because they are simpler and faster than broth-based methods [32, 33].

3. Results and discussion

All prepared metal chelates are colored, solid and stable toward air and moisture. Analytical results of the complexes are consistent with the proposed molecular formulae and confirm the formation of 1 : 1 (Cu^{2+} : L) complexes (table 1).

3.1. *Conductance measurements*

The observed molar conductances ($\Lambda_M = 8.22$–$11.32\ \Omega^{-1}\,cm^2\,mol^{-1}$) of all complexes in 10^{-3} mol L^{-1} DMF solution are given in table 1, revealing their non-electrolytic nature [14]. Such non-zero conductances are probably due to the strong donor capacity of DMF, which may lead to displacement of the anionic ligand and change of the electrolyte type [34].

3.2. *ESI-mass spectra*

The constitutions and purities of the prepared Cu(II)-complexes are confirmed using ESI mass spectrometry. The mass spectra of $[CuL^1(SO_4)]\cdot C_2H_5OH$, $[CuL^2(SO_4)]$, and $[CuL^4(SO_4)(H_2O)_2]\cdot 8H_2O$ showed peaks at m/z 454.4, 454.3, and 657.9, respectively, corresponding to the molecular weight of the parent ion $[ML]^+$. Molecular ion peaks are observed at m/z 657.9, 507.1, and 533.7 in the spectra of $[CuL^3(SO_4)]\cdot 5H_2O$, $[CuL^5(SO_4)]\cdot H_2O\cdot C_2H_5OH$, and $[CuL^6(SO_4)]\cdot 2H_2O$ corresponding to $[ML+1]^+$, whereas $[CuL^7(SO_4)]\cdot C_2H_5OH$ displayed a peak at m/z 531.0 due to $[M+2]^+$. These assignments are based on ^{65}Cu. A further confirmation for the molecular structure of the investigated complexes comes from the appearance of other peaks containing ^{63}Cu besides the peaks due to successive degradation of the target compound to various fragments [20]. For example, the mass spectrum of **4** displayed peaks at m/z 657.9, 655.9, 618.9, 616.9, 585.8, 583.8, 495.0, 493.0, 477.8, and 475.8 corresponding to

Table 1. Physical characteristics, analytical and molar conductance data of the complexes.

No.	Compound (Empirical formula)	Color (Λ_m)	M.Wt. (Cal. M.Wt.)	Elemental analysis			
				%C	%H	%N	%M
1	$[CuL^1(SO_4)]\cdot C_2H_5OH$ ($C_{17}H_{17}CuN_3O_6S$)	Faint green (8.22)	454.40 (453.94)	37.21 (37.54)	4.21 (3.78)	9.55 (9.26)	14.15 (14.00)
2	$[CuL^2(SO_4)]$ ($C_{15}H_{10}CuN_4O_7S$)	Faint green (10.24)	454.30 (453.87)	39.24 (39.70)	2.87 (2.22)	12.54 (12.34)	14.22 (14.00)
3	$[CuL^3(SO_4)]\cdot 5H_2O$ ($C_{15}H_{19}Br_2CuN_3O_{10}S$)	Faint blue (9.26)	657.90 (656.74)	27.59 (27.43)	3.44 (2.92)	6.64 (6.40)	10.11 (9.68)
4	$[CuL^4(SO_4)(H_2O)_2]\cdot 8H_2O$ ($C_{15}H_{29}C_{l2}CuN_3O_{15}S$)	Faint blue (8.44)	657.90 (657.92)	27.62 (27.38)	4.91 (4.44)	7.63 (7.30)	9.89 (9.66)
5	$[CuL^5(SO_4)]\cdot H_2O\cdot C_2H_5OH$ ($C_{17}H_{18}CuFN_3O_8S$)	Faint blue (7.88)	507.10 (505.94)	40.65 (40.36)	3.92 (3.59)	8.75 (8.31)	12.99 (12.56)
6	$[CuL^6(SO_4)]\cdot 2H_2O$ ($C_{15}H_{13}CuN_5O_{11}S$)	Yellow (11.32)	533.70 (534.90)	32.99 (33.68)	2.84 (2.45)	13.50 (13.09)	11.43 (11.88)
7	$[CuL^7(SO_4)]\cdot C_2H_5OH$ ($C_{18}H_{18}CuN_4O_9S$)	Faint blue (10.55)	531.00 (528.96)	41.22 (40.87)	3.81 (3.43)	11.00 (10.59)	12.46 (12.01)

All the synthesized complexes decompose without melting above 220°C. M.Wt. = molecular weight obtained from mass spectral measurements; Cal. M.Wt. = calculated molecular weight; Λ_m = molar conductance ($\Omega^{-1}\,cm^2\,mol^{-1}$).

$[^{65}CuL^4(SO_4)(H_2O)_2]\cdot 8H_2O$, $[^{63}CuL^4(SO_4)(H_2O)_2]\cdot 8H_2O$ (the molecular weight of complex cation), $[^{65}CuL^4(SO_4)(H_2O)_2]\cdot 6H_2O$, $[^{63}CuL^4(SO_4)(H_2O)_2]\cdot 6H_2O$ (loss of two hydrated water molecules), $[^{65}CuL^4(SO_4)(H_2O)_2]\cdot 4H_2O$, $[^{63}CuL^4(SO_4)(H_2O)_2]\cdot 4H_2O$ (loss of four hydrated water molecules), $[^{65}CuL^4(SO_4)(H_2O)_2]$, $[^{63}CuL^4(SO_4)(H_2O)]$ (loss of eight hydrated and one coordinated water molecules), $[^{65}CuL^4(SO_4)]$ and $[^{63}CuL^4(SO_4)]$ (loss of all water molecules). Complexes **1–7** decompose *via* abstraction of the ligand giving ions attributable to $[L]^+$ besides other peaks due to different fragmentation processes of the complexes [35]. The results of both elemental analyses and MS of the prepared complexes are in agreement and confirm the proposed molecular formula (table 1).

3.3. *IR spectral studies*

The mode of bonding in the complexes was investigated by comparison of the IR spectra of the Schiff bases with those of their complexes (table 2). IR spectra of the Schiff bases showed an absorption at 1602–1591 cm^{-1} due to azomethine; the frequency shifted by 4–31 cm^{-1} in the spectra of complexes, suggesting coordination through azomethine nitrogen [36]. The ν(C=N) of the ring appears at 1662–1646 cm^{-1}. The shift by 3–19 cm^{-1} revealed the coordination of the C=N of ring to copper. These observations are supported by a new band at 451–406 cm^{-1}, tentatively assigned to ν(M–N) [37, 38]. IR spectra of all complexes show new bands at 1144–1121, 1095–1021, and 1010–980 cm^{-1}, from bidentate sulfate (figure 2) [14, 39]. A broad band at 3333–3293 cm^{-1} in spectra of hydrated complexes is due to ν(OH) of water or ethanol attached to Cu(II).

3.4. *^{1}H-NMR spectra*

^{1}H-NMR spectra of the free ligands are compared with that of their Cu(II)-complexes **1–7** (table 2). ^{1}H-NMR spectra of L^1–L^7 exhibit a multiplet at 6.28–8.39 ppm for hydrogens of the aromatic rings. In spectra of Cu(II)-complexes, these peaks shift downfield, attributed to increased conjugation on coordination [20]. The azomethine proton (–C<u>H</u>=N–) appeared as a singlet at 8.68–10.45 ppm in free ligands and are strongly downfield shifted upon complex formation, supporting participation of the azomethine nitrogen in coordination to copper. Similar ^{1}H-NMR spectral studies of paramagnetic complexes have been advanced by Wang and Ma [40] in their reports on paramagnetic Cu(II)-complexes. ^{1}H-NMR spectral studies of paramagnetic Fe(II)-complexes have been reported by Wu *et al.* [41, 42]. Also, Khedr and Draz [20] have studied the ^{1}H-NMR spectra of paramagnetic Mn(II)-, Co(II)-, Ni(II)-, and Cu(II)-complexes.

3.5. *ESR, UV-Vis spectra, and magnetic moment measurements*

Based on hyperfine and super hyperfine structures, the ESR spectrum of metal complexes provides information about the geometry and nature of the ligating sites of the Schiff base. The ESR spectra of **3**, **4**, and **6** were recorded at room

Table 2. IR and ^{1}H-NMR, UV-Vis, ESR spectra and magnetic moment data of the ligands and their Cu(II)-complexes.

	IR spectra (cm^{-1})					^{1}H-NMR spectra (ppm)		UV-Vis spectra (d–d transition)		ESR spectra			
Compound	$\nu(H_2O)$ or ν(EtOH)	ν(C=N) (ring)	ν(C=N) (imine)	$\nu(SO_4)$ (bidentate)	ν(M–N)	$\delta_{Ar-\underline{H}}$	$\delta_{\underline{CH}=N}$	Nujol mull	DMSO	$g_{\|\|}$	$g_{\perp}$	g_{eff}	μ_{eff}(B.M.)
L^1	–	1652	1591	–	–	7.24–7.99	10.23	–	–	–	–	–	–
1	3302	1665	1600	1131, 1059, 989	405	7.17–7.80	–	14492	14490	–	–	–	1.70
L^2	–	1647	1597	–	–	6.47–7.98	10.24	–	–	–	–	–	–
2	–	1666	1616	1128, 1059, 986	406	7.17–7.79	–	13986	13985	–	–	–	1.72
L^3	–	1651	1597	–	–	7.31–7.87	10.01	–	–	–	–	–	–
3	3293	1660	1598	1141, 1095, 998	420	7.43–7.80	–	14285	14283	2.01	1.58	1.93	1.69
L^4	–	1653	1596	–	–	7.32–7.89	8.68	–	–	–	–	–	–
4	3300	1666	1565	1132, 1060, 1010	435	6.93–7.87	–	16667	16665	–	–	1.91	1.78
L^5	–	1662	1597	–	–	6.28–8.04	9.77	–	–	–	–	–	–
5	3314	1659	1599	1121, 1059, 980	428	7.32–7.84	–	13888	13886	–	–	–	1.71
L^6	–	1646	1598	–	–	6.50–7.98	10.45	–	–	–	–	–	–
6	3333	1656	1614	1144, 1095, 992	451	7.61–7.78	–	13888	13886	2.08	1.83	1.90	1.70
L^7	–	1658	1602	–	–	7.03–8.39	10.13	–	–	–	–	–	–
7	3320	1663	1605	1121, 1021, 990	440	7.00–7.79	–	13888	13887	–	–	–	1.72

– = Not determined.

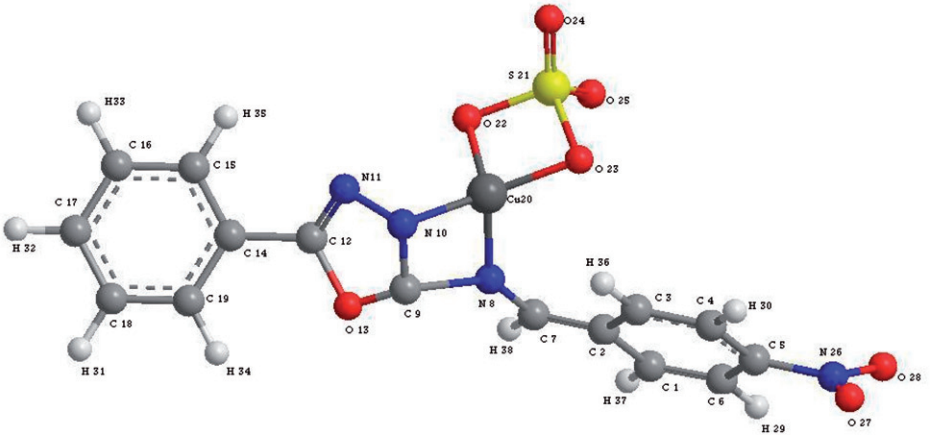

Figure 2. 3-D molecular structure of $[CuL(SO_4)]$ (**2**).

temperature (Supplementary material). The shift of the signal in the low-field region to slightly lower value indicates stronger metal–ligand bonding [43]. Compounds **3** and **6** showed two peaks, one in the low-field region and the other in the high-field region, from which $g_{||}$ and $g_{\perp}$ were calculated (table 2). The $g_{||}$ values (<2.3) indicate covalent character of the metal–ligand bonds [44]. The covalent nature of the metal–ligand bond in the complex is further supported by the g_{eff} value [45], which was <2.0023. The value $g_{||} > g_{\perp}$ is consistent with a primarily $d_{x^2-y^2}$ groundstate [46]. The $d_{x^2-y^2}$ groundstate is characteristic of square planar, square pyramidal, tetrahedral, or octahedral stereochemistry [47]. The $g_{||}/A_{||}$ value can be used to determine the stereochemistry of the copper(II) complex [48]. The range reported for square-planar complexes is 105–135 cm^{-1} and for tetrahedrally distorted complexes is 150–250 cm^{-1}. $g_{||}/A_{||}$ values are 233 and 260 cm^{-1} for **3** and **6**, respectively, in the range expected for distorted tetrahedral complexes. The ESR spectra of the other Cu(II)-complexes display a small broad signal. The g_{eff} value (1.9100 B.M.) and the shape of the signal of the ESR spectra for **4** indicate distorted octahedral geometry [19]. The negative deviation of g_{eff} from the value of the free electron ($g_{\text{eff}} = 2.0023$) may be attributed to covalent bond between Cu(II) and the ligand [19]. The apparent broadening of the ESR signal can be due to antiferromagnetic interaction of Cu–Cu ions. Electronic absorption spectra of **1**–**7** were scanned in Nujol mull and DMSO (table 2). The small change in band position on going from Nujol mull to DMSO indicated that the complexes remain intact in DMSO and the metal ion environments do not differ in the solid state from that in the solution. Except for **4**, spectra displayed bands at 13,888–14,492 cm^{-1} assigned to $^2T_2 \rightarrow {}^2E$ assuming tetrahedral geometry around Cu(II). The electronic spectrum of **4** displays a band at 16,667 cm^{-1} in Nujol mull (at 16,665 cm^{-1} in DMSO) assigned to $^2E_g \rightarrow {}^2T_{2g}$ in distorted octahedral geometry [49]. Cu(II)-complex **4** showed a magnetic moment 1.78 B.M., slightly higher than the spin-only value 1.73 B.M. expected for one unpaired electron, which offers possibility of an octahedral geometry [50]. The room temperature magnetic moment of Cu(II) complexes (table 2) equal 1.69–1.78 B.M. almost agree with the spin only value of 1.73 for $S = ½$, as usually observed for Cu(II) complexes.

Table 3. Thermal analyses (DTA and TGA) of **1**–**7**.

No.	Thermal process	Temp. range (°C)	DTA peaks	TGA (% weight) Found	TGA (% weight) Calcd
1	Loss of ethanol molecule.	100–110	Endo.	9.66	10.15
	Complex decomposition and formation of CuO_2.	475–540	Exo.	20.07	21.05
2	Formation of CuO_2.	650–700	Exo.	20.79	21.05
3	Evaporation of five hydrated water molecules.	80–95	Endo.	13.25	13.72
	Complex decomposition and formation of CuO.	550–650	Exo.	12.06	12.11
4	Evaporation of eight hydrated water molecules.	90–110	Endo.	21.43	21.91
	Loss of two coordinated water molecules.	250–280	Exo.	5.44	5.78
	Complex decomposition and formation of CuO.	550–650	Exo.	12.10	12.09
5	Loss of ethanol and hydrated water molecules.	80–105	Endo.	12.88	12.67
	Complex decomposition and formation of CuO.	420–480	Exo.	15.62	15.72
6	Evaporation of two hydrated water molecules.	95–110	Endo.	7.21	6.74
	Complex decomposition and formation of CuO.	580–640	Exo.	15.00	14.87
7	Loss of ethanol molecule.	95–110	Endo.	9.23	8.71
	Complex decomposition and formation of CuO.	680–720	Exo.	15.06	15.04

3.6. *Thermal analyses (DTA and TGA)*

Thermal analyses have been used to confirm the molecular structure of the complexes. Thermal analyses data are collected in table 3. The DTA curves of the hydrated complexes exhibited broad endothermic peaks at 80–110°C due to the elimination of hydrated water [51]. Coordinated water molecules in **4** are stable displaying an exothermic peak at 250–280°C [52]. Exothermic peak at 420–720°C is attributed to the complete decomposition of the complexes and the formation of copper oxide as a final product. The TGA of the complexes displayed loss of weight from 80 to 110°C corresponding to the loss of ethanol or water. The TGA data are in conformity with the peaks appearing at the same temperature ranges in the DTA curves and the thermal analyses are in accord with that of Osman [53].

3.7. *3-D molecular modeling and analysis*

Molecular modeling of $[CuL(SO_4)]$ (**2**) is based on its distorted tetrahedral structure. For convenience of looking over the different bond lengths and bond angles, the various atoms in the compound in question are numbered in Arabic numerals (figure 2). The details of bond lengths and bond angles per the 3-D structure are given in the "Supplementary material".

The molecular modeling for **2** (figure 2) shows angles around copper of 109.4, 109.4, 109.4, 90, 146.4, and 90.0°; these angles do not change for other complexes which indicate the distorted tetrahedral geometry around Cu(II) ion [24, 25], and thus the proposed structure of **2**, as well as of the others, is acceptable.

3.8. *Antimicrobial activity*

The biological and medicinal potency of coordination compounds has been established by antitumor, antiviral, and antimalarial activities, related to the ability of the metal ion to form complexes with ligand containing nitrogen and oxygen donors [54]. Copper is

Table 4. Antimicrobial activities of **1**–**7**.

Compound	Inhibition zone diameter (mm mg^{-1} sample)[a]			
	E. coli (G^-)	*S. aureus* (G^+)	*A. flavus* (fungus)	*C. albicans* (fungus)
Control: DMSO	0.0	0.0	0.0	0.0
Tetracycline (Antibacterial agent)	33.0 ± 0.3	30.0 ± 0.4	–	–
Amphotericin B (Antifungal agent)	–	–	20.0 ± 0.2	20.0 ± 0.1
Complex **1**	14.0 ± 0.3	15.0 ± 0.4	10.0 ± 0.1	12.0 ± 0.2
Complex **2**	16.0 ± 0.4	16.0 ± 0.2	12.0 ± 0.2	13.0 ± 0.3
Complex **3**	14.0 ± 0.2	14.0 ± 0.3	0.0	12.0 ± 0.4
Complex **4**	14.0 ± 0.5	14.0 ± 0.4	0.0	12.0 ± 0.3
Complex **5**	15.0 ± 0.4	15.0 ± 0.5	0.0	12.0 ± 0.2
Complex **6**	13.0 ± 0.3	15.0 ± 0.2	13.0 ± 0.3	14.0 ± 0.3
Complex **7**	14.0 ± 0.2	15.0 ± 0.3	13.0 ± 0.4	13.0 ± 0.5

[a]Each experiment is conducted at least three times.

an essential micronutrient and a co-factor of several enzymes involved in oxidative metabolism: mono-aminoxidase, superoxydismutase, ascorbic acid oxidase, and tyrosinase. The catalytic role of these enzymes is the result of two processes: (a) the reduction of the Cu^{2+} to Cu^{+}; (b) the fixation of the molecular oxygen [55]. Cu^{2+} is involved in the expression of genes for metal-binding proteins [56]. Through aminoxidase, copper interferes in the metabolism of the conjunctive tissue, contributing to the trophicity of vascular sides [57]. Taking into account the daily necessary quantity of Cu(II) in the organism (2–3 mg per day), its distribution and metabolism in the organism and toxicity, numerous simple or complex combinations of copper are used in the treatment of a variety of diseases, including inflammatory processes, cancer, ulcers, nervous system, and heart diseases. The synthesized complexes were screened for their antibacterial activity [58] against *E. coli* (G^-) and *S. aureus* (G^+) and antifungal activity [59] against *A. flavus* and *C. albicans*. The standard drugs, tetracycline and amphotericin B, were also tested for their antibacterial and antifungal activities at the same concentration and conditions of the test compounds (table 4). The results of antibacterial activity of **1**–**7** show moderate to good activity against *E. coli* and *S. aureus* when compared with tetracycline. From the antifungal activity studies it is inferred that most complexes show high antifungal activity against *A. flavus* and *C. albicans* when compared to amphotericin B (except complexes **3**–**5** which have no activity against *A. flavus*). The test organisms were chosen as follows: *E. coli* was selected as the backbone of Gram negative bacteria and *S. aureus* was selected to represent Gram positive bacteria. Also, we selected *A. flavus* as a higher fungus which represents multicellular fungi. Similarly, *C. albicans* represent the unicellular fungi; they represent a broad spectrum of test organisms. This means that the obtained data for Cu(II)-complexes prove their usefulness as broad spectrum antimicrobial agents.

4. Conclusion

Seven Cu(II) complexes with Schiff bases derived from 2-amino-5-substituted-aryl-1,3,4-oxadiazole were prepared and characterized. Satisfactory elemental and thermal

analyses, molar conductance, magnetic susceptibility, ESI-mass, IR, ^{1}H-NMR, ESR, and electronic spectral studies suggest tetrahedral geometry in all complexes except for **4**, which is octahedral. The results are supported by 3-D molecular modeling of **2** as a representative compound. The complexes were active against the tested bacterial and fungal strains.

Acknowledgments

The authors thank Dr Mohamed El-Zarie (Gakushuin University, Japan) for assistance in measuring ^{1}H-NMR and mass spectra carried out in this work.

References

[1] V.J. Ram. *Indian J. Chem.*, **27**, 825 (1998).
[2] G.S. Ponticello, E.L. Engelhardt, J.J. Baldwin. *Indian J. Heterocycl. Chem.*, **17**, 425 (1980).
[3] G. Sahin, E. Palaska, M. Ekizoglu, M. Ozalp. *Farmacia*, **57**, 539 (2002).
[4] T. Ramalingam, A.A. Deshmukh, P.B. Sattur, U.K. Sheth, S.R. Naik. *J. Indian Chem. Soc.*, **26**, 58 (1981).
[5] S. Holla, C.S. Prasanna, B. Poojary, K.S. Rao, K. Shridhara. *U.G. Bhat. Indian J. Chem.*, **43**, 864 (2004).
[6] D.N. Dhar, C.L. Taploo. *J. Sci. Ind. Res.*, **41**, 501 (1982).
[7] N. Hou, L.J. Xu, Y.H. Pao. *Medline*, **27**, 732 (1992).
[8] S.N. Pandeya, D.S. Ram, G. Nath, E.D. Cleri. *Arzneimittel Forschung*, **50**, 55 (2000).
[9] H. Pavlov, D.J. Litina, A.A. Geronikaki. *Drug Des. Discovery*, **15**, 199 (1997).
[10] S.K. Sridhar, A. Ramesh. *Biol. Pharm. Bull.*, **24**, 1149 (2001).
[11] X. Zhou, L. Shao, Z. Jin, J. Liu, H. Dai, J. Fang. *Heteroatom Chem.*, **18**, 55 (2007).
[12] B.S. Holla, B. Veerendra, M.K. Shivananda, B. Poojary. *Eur. J. Med. Chem.*, **38**, 759 (2003).
[13] P.A. Vigato, S. Tamburini. *Coord. Chem. Rev.*, **248**, 1717 (2004).
[14] T. Rosu, S. Pasculescu, V. Lazar, C. Chifiriuc, R. Cernat. *Molecules*, **11**, 904 (2006).
[15] A. Vogt, S. Wolowiec, R.L. Prasad, A. Gupta, J. Skarzewski. *Polyhedron*, **17**, 1231 (1998).
[16] S. Mehmet, L. Abdulkadir, S. Memet. *Synth. React. Inorg. Met.-Org. Chem.*, **33**, 1747 (2003).
[17] W.M. Laidlaw, R.G. Denning, T. Verbiest, E. Chauchard, A. Persons. *Nature*, **363**, 59 (1994).
[18] M.H. Ali, S.E. Livingstone. *Coord. Chem. Rev.*, **13**, 101 (1974).
[19] R.M. Issa, S.A. Azim, A.M. Khedr, D.F. Draz. *J. Coord. Chem.*, **62**, 1859 (2009).
[20] A.M. Khedr, D.F. Draz. *J. Coord. Chem.*, **63**, 1418 (2010).
[21] A.M. Khedr, S. Jadon, S. Kumar, S. Yadav, V. Kumar, K.C. Gupta. *Asian J. Chem.* (2011) (in press).
[22] A.I. Vogel. *A Text Book of Quantitative Inorganic Analysis*, Longmans, London (1969).
[23] M. Carcelli, S. Ianelli, P. Pelogatti, G. Pelizzi, D. Rogolino, C. Solians, M. Tegoni. *Inorg. Chim. Acta*, **358**, 903 (2005).
[24] CS Chem 3D Ultra Molecular Modeling and Analysis, Cambridge. Available online at: www.cambridgesoft.com (accessed August 15, 2010).
[25] R.C. Maurya, S. Rajput. *J. Mol. Struct.*, **794**, 24 (2006).
[26] A.W. Bauer, W.M. Kirby, C. Sherris, M. Turck. *Am. J. Clin. Path.*, **45**, 493 (1966).
[27] M.A. Pfaller, L. Burmeister, M.A. Bartlett, M.G. Rinaldi. *J. Clin. Microbiol.*, **26**, 1437 (1988).
[28] National Committee for Clinical Laboratory Standards. Performance antimicrobial susceptibility of Flavobacteria, 41 (1997).
[29] National Committee for Clinical Laboratory Standards. Reference method for broth dilution antifungal susceptibility testing of conidium-forming filamentous fungi: Proposed Standard M38-A. NCCLS, Wayne, PA, USA (2002).
[30] National Committee for Clinical Laboratory Standards. Method for antifungal disk diffusion susceptibility testing of yeast: Proposed Guideline M44-P. NCCLS, Wayne, PA, USA (2003).
[31] National Committee for Clinical Laboratory Standards. Methods for dilution antimicrobial susceptibility tests for bacteria that grow aerobically. Approved standard M7-A3. National Committee for Clinical Laboratory Standards, Villanova, PA, USA (1993).

[32] L.D. Liebowitz, H.R. Ashbee, E.G.V. Evans, Y. Chong, N. Mallatova, M. Zaidi, D. Gibbs. *Diagn. Microbiol. Infect. Dis.*, **4**, 27 (2001).
[33] M.J. Matar, L. Ostrosky-Zeichner, V.L. Paetznick, J.R. Rodriguez, E. Chen, J.H. Rex. *Antimicrob. Agents Chemother.*, **47**, 1647 (2003).
[34] S.F.A. Kettle. *Coordination Compounds*, Thomas Nelson & Sons, Nashville, TN (1969).
[35] B.K. Singh, P. Mishra, B.S. Garg. *Transition Met. Chem.*, **32**, 603 (2007).
[36] V. Shrivastava, S.K. Shrivastava, A.P. Mishra. *J. Indian Chem. Soc.*, **22**, 434 (1995).
[37] N. El-Wakeil, A. Khedr, R. Mansour. *Chin. J. Chem.*, **28**, 463 (2010).
[38] R.S. Drago. *Physical Methods in Inorganic Chemistry*, Student Edn, Affiliated East West, Darya Ganj (1978).
[39] K. Nakamato. *Infrared and Raman Spectra of Inorganic and Coordination Compounds*, 4th Edn, John Wiley & Sons, New York (1986).
[40] B. Wang, H. Ma. *Synth. React. Inorg. Met. Org. Chem.*, **34**, 1009 (2004).
[41] W. Wu, D.E. Vanderwall, S.M. Lui, X.J. Tang, C.J. Turner, J.W. Kozarich, J. Stubbe. *J. Am. Chem. Soc.*, **118**, 1268 (1996).
[42] T.E. Lehmann, L.J. Ming, M.E. Rosen, L. Que Jr. *Biochemistry*, **36**, 2807 (1997).
[43] A.S. El-Tabl. *J. Chem. Res.*, **1**, 19 (1981).
[44] D. Kivelson, R. Neeman. *J. Chem. Phys.*, **35**, 149 (1961).
[45] A. Syamal. *Chem. Edu.*, **62**, 143 (1985).
[46] K.K. Narang, V.P. Singh. *Transition Met. Chem.*, **21**, 507 (1996).
[47] M.F. El- Shazly, L.S. Retaat. *Transition Met. Chem.*, **6**, 10 (1981).
[48] A.S. El-Tabl. *Transition Met. Chem.*, **23**, 63 (1998).
[49] H. Liu, H. Wang, F. Gao, D. Niu, Z. Lu. *J. Coord. Chem.*, **60**, 2671 (2007).
[50] D.P. Singh, R. Kumar, V. Malik, P. Tyagi. *Transition Met. Chem.*, **32**, 1051 (2007).
[51] A.P. Mishra, M. Khare, S.K. Gautam. *Synth. React. Inorg. Met-Org. Chem.*, **32**, 1485 (2002).
[52] A.H. Osman, M.S. Saleh, S.M. Mahmoud. *Synth. React. Inorg. Met. Org. Chem.*, **34**, 1069 (2004).
[53] A.H. Osman. *Transition Met. Chem.*, **31**, 35 (2006).
[54] D.L. Kallyman, J.P. Scorill, J.E. Batosevich, J. Bruce. *J. Med. Chem.*, **26**, 35 (1983).
[55] J.A. Halfen, S. Mahapatra, E.C. Wilkinson, S. Kaderli, V.G. Young Jr, L. Que Jr, A.D. Zuberbühler, W.B. Tolman. *Science*, **271**, 1397 (1996).
[56] S.S. Gropper, J.L. Smith, J.L. Groff. *Advanced Nutrition and Human Metabolism*, 4th Edn, Thomson Wadsworth Publishing Co., Belmont, CA (2005).
[57] U. Sakaguchi, A.W. Addison. *J. Am. Chem. Soc.*, **99**, 5189 (1977).
[58] F. Simoncini, R. Rangone, C. Calanni. *Farnance Ed. Prat*, **23**, 559 (1968).
[59] H.W. Seely, P.J. Van Demark. *Microbes in Action, Laboratory of Microbiology*, 3rd Edn, W H Freeman and Co., USA (1981).